

DEVELOPMENT OF BEAM CURRENT MONITOR WITH HTS SQUID AND HTS CURRENT SENSOR

T. Watanabe*, N. Fukunishi, M. Kase, Y. Sasaki and Y. Yano

RIKEN Nishina Center for Accelerator-Based Science, Wako-shi, Saitama 351-0198 Japan

Abstract

A highly sensitive beam current monitor with an HTS (High-Temperature Superconducting) SQUID (Superconducting Quantum Interference Device) and an HTS current sensor, that is, an HTS SQUID monitor, has been developed for use of the RIBF (RI beam factory) at RIKEN. Unlike other existing facilities, the HTS SQUID monitor allows us to measure the DC of high-energy heavy-ion beams nondestructively in real time, and the beam current extracted from the cyclotron can be recorded without interrupting the beam user's experiments. Both the HTS magnetic shield and the HTS current sensor were dip-coated to form a $\text{Bi}_2\text{-Sr}_2\text{-Ca}_2\text{-Cu}_3\text{-O}_x$ (Bi-2223) layer on 99.9% MgO ceramic substrates. In the present work, all the fabricated HTS devices are cooled by a low-vibration pulse-tube refrigerator. These technologies enabled us to downsize the system. Prior to practical use at the RIBF, the HTS SQUID monitor was installed in the beam transport line of the RIKEN ring cyclotron to demonstrate its performance. As a result, a $20 \mu\text{A } ^{40}\text{Ar}^{15+}$ beam intensity (63 MeV/u) was successfully measured with a 500 nA resolution. Despite the performance taking place in an environment with strong gamma ray and neutron flux radiation, RF background and large stray magnetic fields, the measurements were successfully carried out in this study. This year, the HTS SQUID monitor was upgraded to have a resolution of 100 nA and was reinstalled in the beam transport line, enabling us to measure a $4 \mu\text{A } ^{132}\text{Xe}^{20+}$ (10.8 MeV/u) beam and a $1 \mu\text{A } ^{132}\text{Xe}^{41+}$ (50.1 MeV/u) beam used for the accelerator operations at RIBF.

Hence, we will report the results of the beam measurement and the present status of the HTS SQUID monitor.

INTRODUCTION

The RIBF project to accelerate all elements from hydrogen to uranium up to an energy of 440 MeV/u for light ions and 350 MeV/u for heavy ions started in April 1997 [1]. Fig. 1 shows a schematic layout of the RIBF facility. These research activities in the RIBF project make extensive use of the heavy-ion accelerator complex, which consists of one linac and four ring cyclotrons, i.e., a variable-frequency linac (RILAC), the RIKEN ring cyclotron (RRC), a fixed-frequency ring cyclotron (fRC), an intermediate-stage ring cyclotron (IRC) and a superconducting ring cyclotron (SRC). Energetic heavy-ion beams are converted into intense RI beams via the projectile frag-

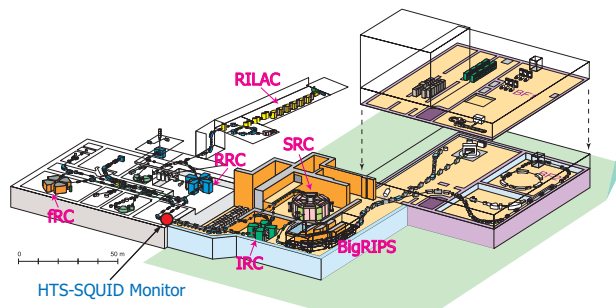


Figure 1: Schematic bird's-eye view of the RIBF facility.

mentation of stable ions or the in-flight fission of uranium ions using a superconducting isotope separator, BigRIPS [2]. The combination of these accelerators and BigRIPS will greatly expand our knowledge of the nuclear world into the presently inaccessible region on the nuclear chart. We succeeded in accelerating a uranium beam to 345 MeV/u in March 2007, and a new RI, a neutron-rich palladium isotope, ^{125}Pd , was discovered in July 2007 [3, 4].

Hence, it is essential to keep the beam transmission efficiency as high as possible, because the production of the RI beam requires an intense primary beam during the beam commissioning. Furthermore, activation produced by beam loss, in particular, should be avoided. In this facility, to evaluate the beam transmission efficiency, Faraday cups are used. When an accelerated particle collides with the surface of a Faraday cup, secondary electrons are always generated. If these electrons escape from the insulated cup area, the reading of the beam current is wrong by the number of lost electrons. Thus, the suppression of secondary electrons is very important for measuring the beam current precisely. Usually, this can be done by applying a high negative voltage close to the entrance of the cup. However, since the electrical field on the beam axis is lower than that on the edge, it is difficult to completely suppress the high-energy secondary electrons that are produced by high-energy heavy-ion beams such as uranium beams. To evaluate how many secondary electrons are generated by a beam, a high positive voltage was used for suppression. A measurement result obtained by applying the suppression voltage for a $10.7 \text{ MeV/u } ^{238}_{92}\text{U}^{72+}$ beam is shown in Fig. 2. From this result, the current generated by the secondary electrons was found to be eight times stronger than that of the uranium beam.

To resolve this technical issue, a study of the HTS SQUID monitor has been started at RIKEN [5, 6, 7].

*wtamaki@riken.jp

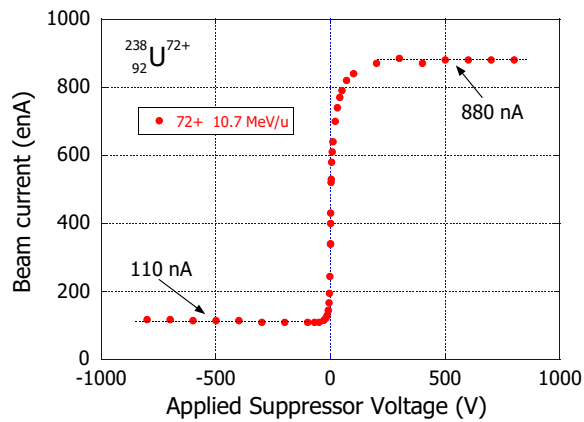


Figure 2: Measurement result obtained applying suppression voltage for 10.7 MeV/u $^{238}_{92}\text{U}^{72+}$ beam. To evaluate how many secondary electrons are generated by the beam, a positive high voltage was used for suppression.

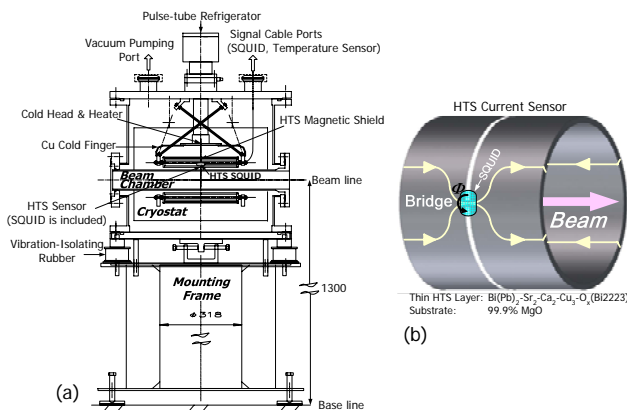


Figure 3: Schematic drawing of the HTS SQUID monitoring system (a) and the current sensor (b).

HTS SQUID MONITOR SYSTEM

A schematic drawing of the HTS SQUID monitor system is shown in Fig. 3(a). This system consists of two vacuum chambers completely separated from each other: one for a cryostat in which the HTS SQUID, an HTS magnetic shield and an HTS current sensor are cooled, and the other the chamber that a beam passes through. In the present work, all these fabricated HTS devices are cooled by a low-vibration pulse-tube refrigerator with a refrigeration power of 11 W at a temperature of 77 K. The operation temperature can be set in the range of 64 K to 90 K (the critical temperature of the HTS SQUID) using a heater, since the pulse-tube refrigerator is capable of cooling the system to temperatures lower than liquid-nitrogen temperature. Furthermore, it is possible to stabilize the temperature of the HTS SQUID with an accuracy of 5 mK using a PID feedback controller, which has four thermometers and a heater. The PID controller calculation involves three separate pa-

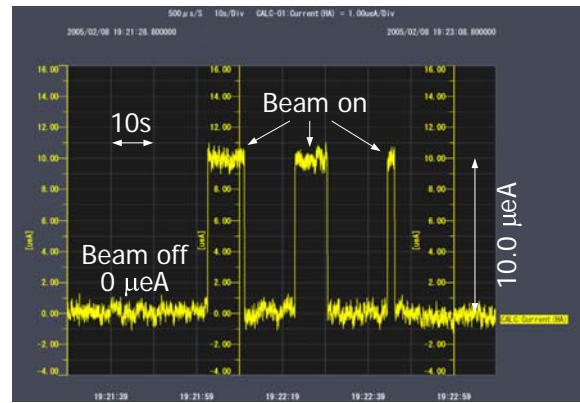


Figure 4: A $10\ \mu\text{A}$ $^{40}\text{Ar}^{15+}$ beam intensity (63 MeV/u) was successfully measured in real-time with a 500 nA resolution when a $1\ \mu\text{A}$ beam produced a magnetic flux of $6.5 \times 10^{-6} \Phi_0$ at the input coil of the HTS SQUID.

rameters; the Proportional, the Integral and Derivative values. The temperature of the cold head was measured as a function of time. Consequently, the deviation of the temperature over a period of 18 h was controlled within 3.4 mK (1σ) [5]. Both the HTS magnetic shield and the HTS current sensor were fabricated by dip-coating a thin $\text{Bi}_2\text{-Sr}_2\text{-Ca}_2\text{-Cu}_3\text{-O}_x$ (Bi-2223) layer on 99.9% MgO ceramic substrates. The HTS SQUID system (Model BMS-G manufactured by Tristan Technologies) contains a low-noise HTS SQUID gradiometer ($\text{Y-Ba}_2\text{-Cu}_3\text{O}_{7-\delta}$) and a controller [5]. When a charged particle (ion or electron) beam passes along the axis of the HTS tube, a shielding current produced by the Meissner effect flows in the opposite direction along the wall of the HTS tube so as to screen the magnetic field generated by the beam. Since the outer surface is designed to have a bridge circuit (Fig. 3(b)), the current generated by the charged particle beam is concentrated in the bridge circuit and forms an azimuthal magnetic field Φ around the bridge circuit. The HTS SQUID is set close to the bridge circuit and can detect the azimuthal magnetic field with a high S/N ratio.

EXPERIMENTAL RESULTS

Prior to the beam measurements in the RRC hall, preliminary measurements were successfully carried out as follows: (1) the first beam test of the HTS SQUID monitor in the beam transport line for the electron cyclotron resonance (ECR) ion source in the CNS experimental hall and (2) the second beam measurement at the E1 experimental hall in RIKEN to measure the current of the high-energy heavy-ion beam. Aiming at practical use for accelerator operations, the authors installed the HTS SQUID monitor system in the beam transport line in the RRC hall (Fig. 1).

However, the SQUID electric circuit, which has a dynamic range of 100 dB (from $1\ \mu\text{A}$ to 0.1 A) and a frequency range from DC to 25 kHz, did not function normally owing to the following reasons: (1) an RF back-

ground was caused by the high-power RF cavities of the RRC, which can produce a total power of 0.6 MW; (2) a large stray magnetic field was induced by the main magnetic field of the RRC (max. 1.67 T); (3) there was a neutron radiation dose of 25.5 Sv/year and a gamma radiation dose of 3.0 Sv/year. The radiation doses of neutrons and gamma rays were measured using an ionization chamber and a ^3He proportional counter, respectively. The actual radiation doses where the HTS SQUID monitor is installed should be higher than the above values, because both dosimeters are located 4 m above the HTS SQUID monitor. These data gave tentative criteria from the judgment of safety for radiation damage. After overcoming these difficulties by reinforcing the RF shield and surrounding the flux-locked loop (FLL) circuit with lead and concrete blocks, there were no more problems with the beam current measurement. As a result, a $10\ \mu\text{A}\ ^{40}\text{Ar}^{15+}$ beam intensity (63 MeV/u) was successfully measured with a 500 nA resolution, as shown in Fig. 4, where a $1\ \mu\text{A}$ beam produced a magnetic flux of $6.5 \times 10^{-3} \Phi_0$ at the input coil of the HTS SQUID.

Futhermore, a prolonged recording 4 h of the Ar beam current extracted from the RRC without interruption of the beam user's experiments was achieved, as shown in Fig. 5(a). In this recording, several dips in beam intensity due to ECR ion source discharge can be observed at irregular intervals of 10 s to 60 min. Fig. 5(b) shows a magnified

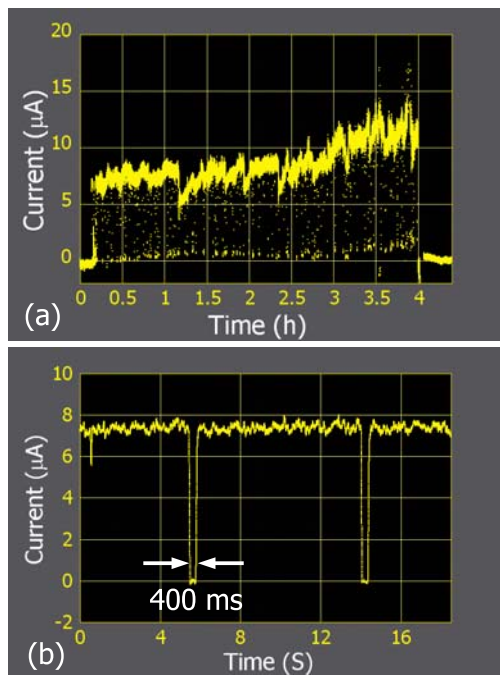


Figure 5: (a) Measurement of 63 MeV/u Ar beam extracted from RRC, which could be recorded for approximately 4 h without interrupting the beam user's experiments. (b) Magnified image of (a) showing dips in current caused by ECR ion source discharge, which recovered within 400 ms.

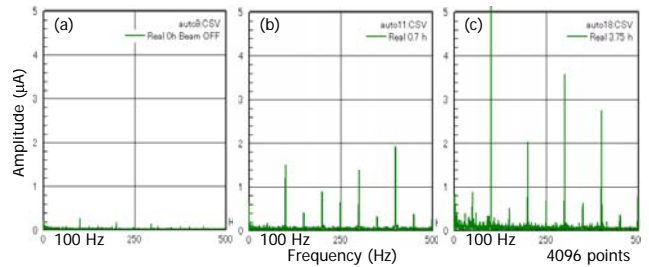


Figure 6: Results analyzed by fast Fourier transform (FFT) of measurements shown in Fig. 5 (a) at 0 h (beam off) (a), 0.7 h (b) and 3.75 h (c).

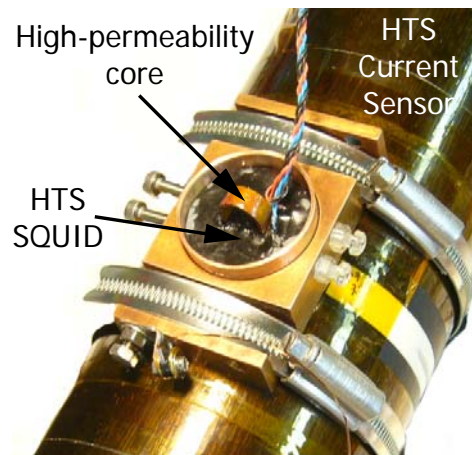


Figure 7: Photograph of new HTS SQUID with two holes containing high-permeability cores.

image of Fig. 5(a), which indicates that the dips in current caused by ECR ion source discharge recovered within 400 ms. The current signals were analyzed by a fast Fourier transform (FFT) in a frequency domain and the results are shown in Fig. 6. The amplitudes of ripples in the modulated beam current increased with beam current. All recording and control systems were connected to a PC-based data acquisition system. Through the Ethernet, these systems were linked to a laptop in the main control room located 200 m from the RRC hall. The sampling time for data acquisition was $500\ \mu\text{s}$, and 100 data points were averaged to improve the signal-to-noise ratio.

PRACTICAL USE OF HTS SQUID MONITOR FOR RIBF

Upgrade and Measurement Results

Aiming at practical use for accelerator operations at the RIBF, we developed a new HTS-SQUID with a high-permeability core that is installed in the two input coils of the HTS-SQUID to improve sensitivity [7]. Fig. 7 shows a photograph of the new HTS SQUID with two holes containing high-permeability cores. The core is composed of

80% Ni and Mo, Re and Fe. The output voltage of the HTS SQUID controller as a function of the simulated beam current is plotted in Fig. 8. From these measurement results, the calibration equation is obtained as

$$\begin{aligned} V_s &= S_{co} \times I_b \times G/500 \\ &= 46.60 \times I_b \times G/500, \end{aligned}$$

where S_{co} , I_b , V_s and G are the coupling efficiency (mV/ μ A), the beam current (μ A), the output voltage of the SQUID controller (mV) and the gain, respectively. A test using a simulated beam current showed a 2-fold improvement in gain, because the coupling efficiency S_{co} of the HTS SQUID monitor when it was not equipped with the magnetic core was 22.8 mV/ μ A [5]. The transfer of the magnetic field produced by the simulated beam current to the SQUID is thus improved. The HTS SQUID monitor was upgraded with the new HTS SQUID and the magnetic core, following which the HTS SQUID monitor was re-assembled. For the purpose of canceling the environmental magnetic noise, the previous mounting frame made of iron was replaced with one made of aluminum with a relative permeability of 1. Fig. 9 shows the HTS SQUID monitor equipped the Al mounting frame and the noise cancellation system, which was installed in the transport line between the fRC and the IRC (Fig. 1). Fig. 10 shows the results of the cooling processes; the temperatures of the cold head, the thermal anchor and the Cu block holding the SQUID were recorded for over 30 h using silicon diode thermometers. The temperature of the HTS SQUID was found to reach the temperature of liquid nitrogen (77 K) after 16.5 h. This year, we were able to measure a 3.6 μ A $^{132}\text{Xe}^{20+}$ (10.8 MeV/u) beam (Fig. 11) and a 1 μ A $^{132}\text{Xe}^{41+}$ (50.1 MeV/u) beam for use in the accelerator operations at RIBF as a result.

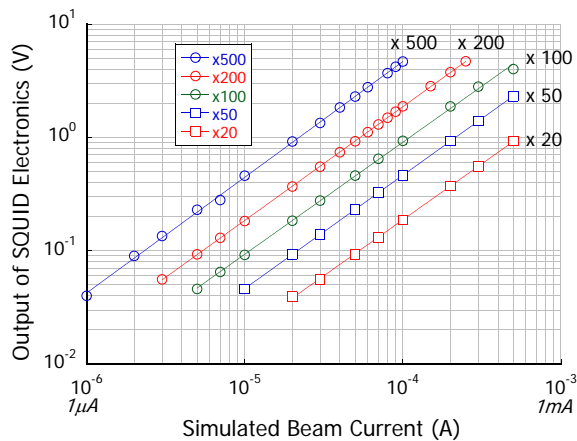


Figure 8: Plot of output voltage of the HTS SQUID controller as a function of simulated beam current.

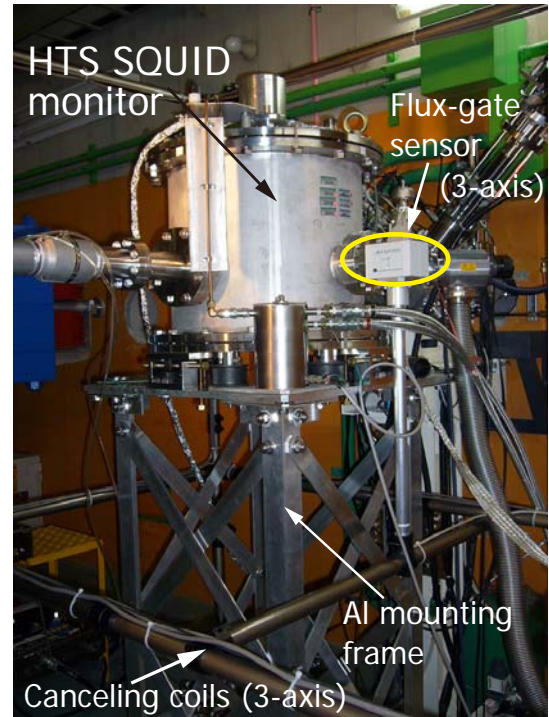


Figure 9: HTS SQUID monitor equipped with the Al mounting frame and the noise cancellation system, which was installed in the transport line between the fRC and the IRC (Fig. 1).

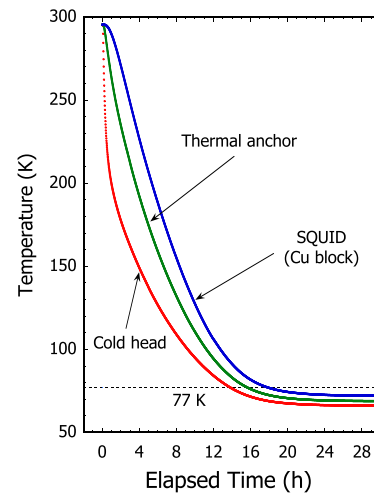


Figure 10: Cooling processes recorded for over 30 h using silicon diode thermometers.

Noise Reduction

To obtain a better resolution for the measurement, we paid close attention to the reductions of noise. A noise-cut transformer, which is completely isolated from the power circuit and not affected by AC source noise, was introduced to remove normal-mode and common-mode noises. In line noise, the noise that flows along one line of leading wires

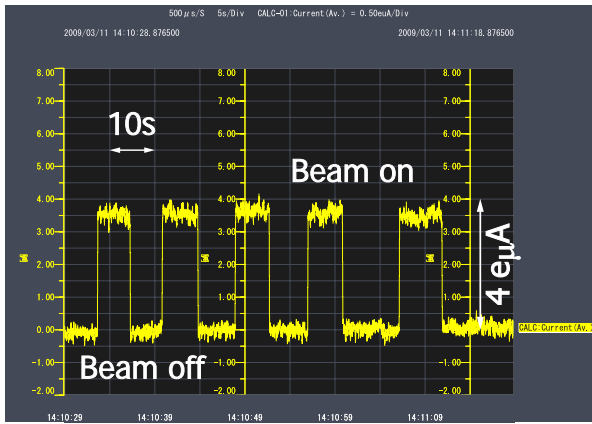


Figure 11: This year, we were able to measure a $3.6 \mu\text{A}$ $^{132}\text{Xe}^{20+}$ (10.8 MeV/u) beam.

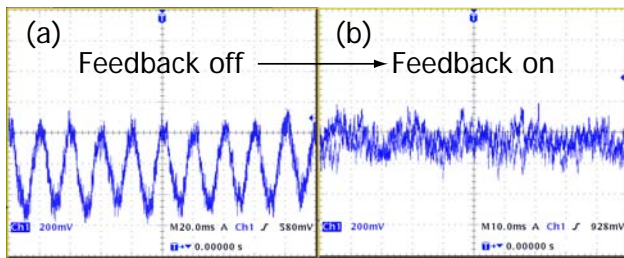


Figure 12: Effect of removed environmental noise by introducing the noise cancellation system.

in one direction and then another line in the return journey is called normal-mode noise, and the noise that flows along both lines in the outward journey and to earth in the return journey is called common-mode noise. Furthermore, all instruments are fixed on a large aluminum plate and the grounds of the instruments are connected to the plate. The signal cables were wired carefully to reduce unnecessary loops as much as possible and all AC lines were covered by braided wires.

The design of noise cancellation system is based on a three-axis Helmholtz cage and feedback control engineering. Three-axis flux-gate sensors are placed near the equipment. A signal is fed through the proprietary controller to a compensation coil, producing precisely calibrated electromagnetic fields. The preliminary result in Figs. 12 (a) and (b) shows the effect of the removal of environmental noise by introducing the noise cancellation system.

The data acquisition and control program, being written in LabVIEW (National Instruments, Ltd.), is almost complete, but some modifications are necessary.

The authors are grateful to E. Nemoto of JEOL DATUM, Ltd., for cooperation regarding the noise cancellation system.

REFERENCES

- [1] Y. Yano, Nucl. Instrum. and Meth. (2007) B 261 p. 1009.
- [2] T. Kubo et al., IEEE Trans. Appl. Supercond. 17 (2003) p. 97.
- [3] Y. Yano, Proc. Int. Nuclear Physics Conf. (INPC2007), Tokyo, Japan, June 2007; Proc. 22nd Particle Accelerator Conf. 07 (PAC07), Albuquerque, New Mexico, U.S.A., June 2007.
- [4] T. Ohnishi et al., J. Phys. Soc. Jpn. 77 No.8 (2008) p. 1069.
- [5] T. Watanabe T et al., Supercond. Sci. Technol. 17 (2004) S450.
- [6] T. Watanabe et al., J. Phys. 43, (2006) p. 1215.
- [7] T. Watanabe et al., J. Phys. 97, (2008) p. 012248.